

Effects of nanowire coalescence on their structural and optical properties on a local scale

V. Consonni,^{a)} M. Knelangen, U. Jahn, A. Trampert, L. Geelhaar, and H. Riechert
Paul-Drude-Institute for Solid State Electronics, Hausvogteiplatz 5-7, 10117 Berlin, Germany

(Received 16 October 2009; accepted 28 November 2009; published online 18 December 2009)

The effects of GaN nanowire coalescence have been investigated on a local scale by combining high-resolution transmission electron microscopy imaging with spatially resolved cathodoluminescence measurements. Coalescence induces the formation of a network of boundary dislocations, above which I_1 -type basal-plane stacking faults are nucleated. The former contributes to the reduction in the crystalline quality at the bottom of coalesced nanowires while the latter leads to intense excitonic radiative transitions at 3.42 eV in their center. Despite coalescence, the top of coalesced nanowires presents a very high crystalline quality, resulting in strong radiative recombinations of donor bound excitons at 3.47 eV. © 2009 American Institute of Physics.
 [doi:10.1063/1.3275793]

In the past decade, semiconductor nanowires (NWs) have received increasing interest due to their high aspect ratio in the nanoscale dimensions and their suitable compatibility with silicon-based technology, opening the way to a wide variety of potential nanodevices.^{1,2} GaN and its alloys are a highly important class of materials for the realization of efficient light emitting diodes (LED),^{3,4} and the NW morphology may lead to further improvements in efficiency or in the reduction of costs.^{5,6} One advantage of this morphology is the very low density of extended defects formed during growth as compared to two-dimensional planar layers of the same material. This originates from the possible strain relaxation through the NW lateral surfaces.⁷ A particularly attractive approach for the fabrication of GaN NWs is the growth by plasma-assisted molecular beam epitaxy (PAMBE), which takes place on silicon substrate in a self-induced way without the use of any external catalyst material or patterning.^{8–10} For many technological applications such as LEDs, solar cells or sensors, the formation of highly dense ensembles of well-separated GaN NWs is required and easily achieved by PAMBE.^{1,2,6–9} However, the high density of these NWs—about 10^{10} cm⁻²—results in an inevitable coalescence process, which could be detrimental for transport and electronic properties.^{8,11–13} In general, any approach to fabricate extremely dense NW ensembles faces this problem. The coalescence process has widely been investigated for polycrystalline materials and commonly induces the formation of numerous extended defects, such as the so-called grain boundaries, as well as the generation of high local tensile stresses.¹⁴ Nevertheless, although such a process has often been mentioned in the case of NWs and especially for self-induced GaN NWs, its precise effects on the structural and optical properties on a local scale are still an open question.^{11–13,15}

In this letter, we study the NW coalescence process and its effects on a local scale by combining high-resolution transmission electron microscopy (HRTEM) imaging and low-temperature cathodoluminescence (CL) measurements. GaN NWs were grown on [111]-oriented silicon substrates

by PAMBE. Atomic nitrogen and gallium atoms were supplied by a plasma source operating at 500 W power with a 2 sccm flux and by a thermal effusion cell operating at 860 °C, respectively. Prior to NW growth, the silicon substrate was exposed to an atomic nitrogen flux for 5 min for nitridation, which results in the formation of a 5 nm thick Si_xN_y amorphous interlayer. GaN NWs were subsequently grown for 3 h at a substrate temperature of 780 °C under highly nitrogen-rich conditions, corresponding to a V/III ratio of about 6. Cross-sectional TEM specimens were prepared by mechanical lapping and polishing, followed by argon ion milling according to standard techniques. HRTEM images were acquired with a JEOL 3010 microscope operating at 300 kV. 6 K CL measurements were carried out with a Zeiss ULTRA55™ field-emission scanning electron microscope equipped with a Gatan mono-CL3™ detector and He-cooling stage system. For the CL excitation, the acceleration voltage and electron beam current were chosen to be 5 kV and about 1 nA, respectively.

The morphology of GaN NWs as well as the typical effects of their coalescence on the structural properties on a local scale are presented in Fig. 1. These NWs are slightly tilted with respect to the substrate by an angle of a few degrees, most likely due to the roughness of the amorphous interlayer. This tilt results in the NW coalescence process, which typically occurs for geometrical reasons at a mean NW length of several hundred nanometers. We point out that two NWs nucleating very closely and slightly twisted with respect to each other may also coalesce without the need of any tilt through their radial growth, although such a process is expected to be a less general coalescence mechanism and thus is not observed in Fig. 1.

First, we systematically observe in all of the studied samples that the tilt between the two misaligned coalesced NWs is accommodated by the formation of a network of boundary dislocations, as revealed in the inset of Fig. 1. Such boundary dislocations can be of pure edge-type with a Burgers vector of **a** in order to accommodate the tilt component.¹⁶ If besides such a component, a twist component exists between the two coalesced NWs as it is expected in our case, boundary dislocations can be of mixed-type with a Burgers vector of **a+c**.¹⁶ The number of boundary disloca-

^{a)}Electronic mail: vconsonni@9online.fr.

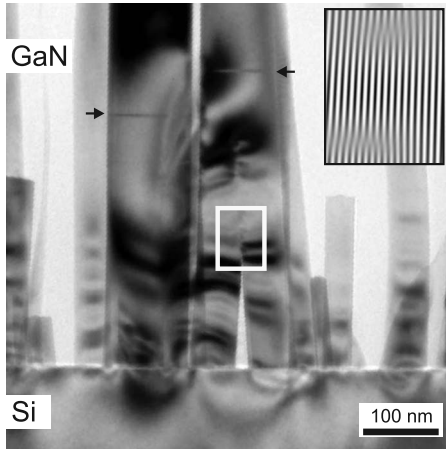


FIG. 1. TEM overview of two coalesced NWs. The black arrows indicate the location of SFs. The white box indicates the location of boundary dislocations just above the contact point. The inset reveals a Fourier-filtered enhancement showing only the $\{1\bar{1}00\}$ lattice planes to emphasize the edge character of the boundary dislocations.

tions involved in the network depends on the local conditions of the coalescence process; more boundary dislocations are likely to be formed with increasing tilt and twist components between the two coalesced NWs. Local stress is further generated around the network of boundary dislocations, as revealed by bend contours in Fig. 1 but is accommodated by the lateral surfaces of the coalesced NWs.

Second, we systematically notice in all of the studied samples the formation of basal-plane stacking faults (SFs) at a mean separation of several hundred nanometers above the contact point between the two coalesced NWs, as shown in Fig. 1. The HRTEM image in Fig. 2 shows a sequence of ABABACACAC planes, indicating that the SF is of I_1 -type.¹⁷ This type of SF is formed during growth but is not generated due to slip and strain relief. The physical origin of its formation has not completely been elucidated yet but its systematic presence in coalesced NWs above the network of boundary dislocations as well as its absence in uncoalesced NWs highlights a clear correlation with the coalescence process. It should be noted however that the I_1 -type basal-plane

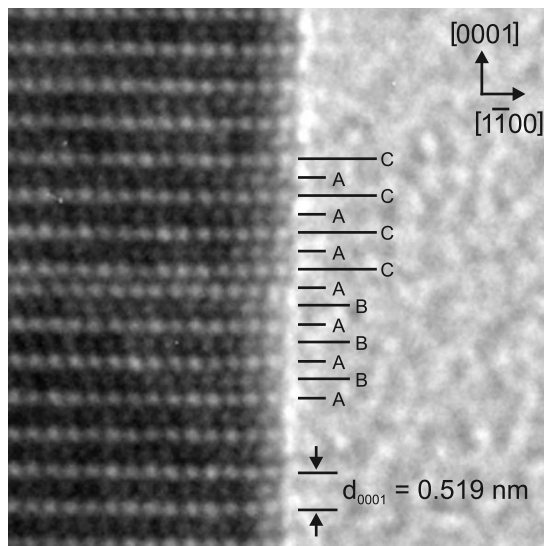


FIG. 2. HRTEM image of a basal-plane SF as marked in Fig. 1. The SF is of I_1 -type and starts on the Aa layer (...ABABACACAC...).

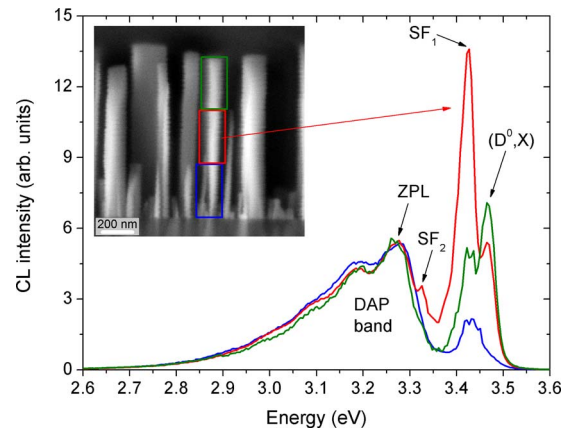


FIG. 3. (Color online) CL spectra recorded at 6 K and excited at the bottom, center, and top of one freestanding coalesced NW. The SEM image in the inset shows the corresponding regions that were analyzed for the CL measurements.

SF has a very low formation energy.¹⁸ Above these SFs, the top of coalesced NWs is free of any type of extended defects that could be observed by HRTEM imaging, which reveals the very high crystalline quality of this NW region.

CL spectra have been recorded at 6 K at the bottom, center, and top of a single freestanding coalesced GaN NW, as presented in Fig. 3. These spectra consist of three types of distinct emissions. Radiative recombinations of bound excitons $[(D^0, X)]$ to silicon or oxygen donors give rise to a line at 3.47 eV.¹⁹ In GaN, silicon and oxygen act as hydrogenic donors by substituting for gallium and nitrogen sites with very close ionization energies of 30.18 and 33.2 meV, respectively.²⁰ We emphasize that the presence of such an intense line in unintentionally doped GaN is a sign of its high crystalline quality. The nature of the line at 3.42 eV remains controversially discussed in the literature. In our case, we associate it with radiative recombinations of excitons bound to I_1 -type basal-plane SFs (SF_1), as evidenced below.^{21,22} Furthermore, a donor-acceptor pair (DAP) band is observed, which is composed of a zero phonon line (ZPL) centered at 3.28 eV followed by two longitudinal optical phonon replicas at 3.19 and 3.10 eV, each separated by a phonon energy of 91.7 meV.²¹

Although all of these three types of emissions appear on all of the three spectra located at the bottom, center, and top of the coalesced NW, we point out that there are major differences concerning the predominant emissions. In Fig. 4, monochromatic CL images of the same single freestanding coalesced GaN NW obtained for varying CL detection energies (i.e., at 3.28, 3.42, and 3.47 eV) clearly confirm that the corresponding luminescence lines predominantly originate from different NW regions.

The intensity of the ZPL corresponding to the DAP band at 3.28 eV remains unchanged along the coalesced NW in Fig. 3 and is homogeneously distributed in Fig. 4(b). This is a strong indication that the spatial distribution of donors and acceptors composing the pairs is uniform. However, the excitonic band is much less intense at the bottom of the coalesced NW than at its center and top for both CL lines at 3.47 and 3.42 eV. Instead, the DAP band dominates the spectrum recorded at the bottom of the coalesced NW, revealing a reduction in its crystalline quality. Boundary dislocations are expected to trap charge carriers or induce their nonradiative

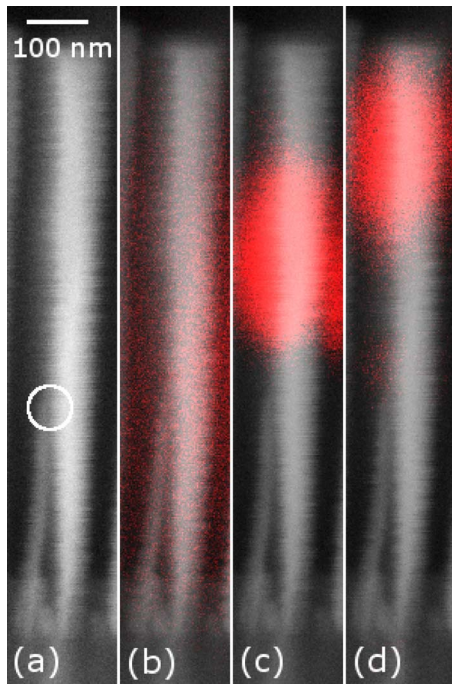


FIG. 4. (Color online) (a) SEM image, [(b)–(d)] SEM and superimposed monochromatic CL images of the same freestanding coalesced NW as shown in Fig. 3. For (b), (c), and (d), the CL detection energy was chosen to be 3.28 eV (ZPL), 3.42 eV (SF_1), and 3.47 eV [(D°, X)], respectively. The white circle in (a) indicates the contact point between the two freestanding coalesced NWs.

recombination, resulting in a drastic decrease in the density of excitons. This, in turn, leads to the low intensity of the excitonic band. In contrast, the excitonic band is much more intense in the spectra recorded at the center and top of the coalesced NW, but the nature of the predominant line varies. At the center, the 3.42 eV (SF_1) line clearly dominates the excitonic band, as revealed in Fig. 3. Figure 4(c) also shows that such a line is much more intense at the center of the coalesced NW. These observations give strong, direct evidence that I_1 -type basal-plane SFs, which have been observed by HRTEM imaging in this region of the coalesced NWs (see Figs. 1 and 2), contribute to the 3.42 eV line by acting as efficient radiative recombination centers.²² In addition, there exists a line at 3.33 eV (SF_2), which is possibly related to the presence of prismatic SFs.²² At the top of the coalesced NW, the (D°, X) line at 3.47 eV has the highest intensity, as shown in Fig. 3. Figure 4(d) reveals that such a line is also much more intense at this region of the coalesced NWs. These findings are in agreement with the absence of extended defects observed in HRTEM images and confirm that, despite coalescence, the crystalline quality at the top of the coalesced NW remains very high.

In conclusion, the process of GaN NW coalescence induces the formation of a network of boundary dislocations and further I_1 -type basal-plane SFs above the contact point. Such a process, in turn, strongly affects the luminescence characteristics of the coalesced GaN NWs. The boundary dislocations contribute to the poor structural and optical quality in the bottom of GaN coalesced NWs whereas the I_1 -type basal-plane SFs dominate the optical properties in their center through the presence of an intense excitonic line at 3.42 eV. Despite coalescence, the top of the coalesced GaN NWs retains a very high crystalline quality free of any type of extended defects, leading to good optical properties governed by an intense excitonic line at 3.47 eV.

This work was partly supported by the German BMBF joint research project MONALISA (Contract No. 01BL0810). The authors are grateful to O. Brandt for fruitful discussions. One of the authors (M.K.) acknowledges funding by the German National Academic Foundation.

¹C. M. Lieber and Z.L. Wang, *MRS Bull.* **32**, 99 (2007).

²M. Law, J. Goldberger, and P. Yang, *Annu. Rev. Mater. Res.* **34**, 83 (2004).

³S. C. Jain, M. Willander, J. Narayan, and R. Van Overstraeten, *J. Appl. Phys.* **87**, 965 (2000).

⁴F. A. Ponce and D. P. Bour, *Nature (London)* **386**, 351 (1997).

⁵H. M. Kim, T. W. Kang, and K. S. Chung, *Adv. Mater.* **15**, 567 (2003).

⁶S. D. Hersee, M. Fairchild, A. K. Rishinaramangalam, M. S. Ferdous, L. Zhang, P. M. Varangis, B. S. Swartzentruger, and A. A. Talin, *Electron. Lett.* **45**, 75 (2009).

⁷E. P. A. M. Bakkers, M. T. Borgström, and M. A. Verheijen, *MRS Bull.* **32**, 117 (2007).

⁸M. Yoshizawa, A. Kikuchi, M. Mori, N. Fujita, and K. Kishino, *Jpn. J. Appl. Phys., Part 2* **36**, L459 (1997).

⁹M. A. Sanchez-Garcia, E. Calleja, E. Monroy, F. J. Sanchez, F. Calle, E. Muñoz, and R. Beresford, *J. Cryst. Growth* **183**, 23 (1998).

¹⁰N. Wang, Y. Cai, and R. Q. Zhang, *Mater. Sci. Eng. R.* **60**, 1 (2008).

¹¹R. Songmuang, O. Landré, and B. Daudin, *Appl. Phys. Lett.* **91**, 251902 (2007).

¹²R. Calarco, R. Meijers, R. K. Deb Nath, T. Stoica, E. Sutter, and H. Lüth, *Nano Lett.* **7**, 2248 (2007).

¹³J. Ristić, E. Calleja, S. Fernández-Garrido, L. Cerutti, A. Trampert, U. Jahn, and K. H. Ploog, *J. Cryst. Growth* **310**, 4035 (2008).

¹⁴W. D. Nix and B. M. Clemens, *J. Mater. Res.* **14**, 3467 (1999).

¹⁵K. A. Bertness, A. Roshko, L. M. Mansfield, T. E. Harvey, and N. A. Sanford, *J. Cryst. Growth* **310**, 3154 (2008).

¹⁶F. A. Ponce, D. Cherns, W. T. Young, and J. W. Steeds, *Appl. Phys. Lett.* **69**, 770 (1996).

¹⁷H. Blank, P. Delavignette, R. Gevers, and S. Amelinckx, *Phys. Status Solidi* **7**, 747 (1964).

¹⁸C. Stampfl, and C. G. Van de Walle, *Phys. Rev. B* **57**, R15052 (1998).

¹⁹E. Calleja, M. A. Sánchez-García, F. J. Sánchez, F. Calle, F. B. Naranjo, E. Muñoz, U. Jahn, and K. Ploog, *Phys. Rev. B* **62**, 16826 (2000).

²⁰W. J. Moore, J. A. Freitas, Jr., S. K. Lee, S. S. Park, and J. Y. Han, *Phys. Rev. B* **65**, 081201 (2002).

²¹M. A. Reshchikov and H. Morkoç, *J. Appl. Phys.* **97**, 061301 (2005).

²²R. Liu, A. Bell, F. A. Ponce, C. Q. Chen, J. W. Yang, and M. A. Khan, *Appl. Phys. Lett.* **86**, 021908 (2005).